Int. J. Heat Mass Transfer. Vol. 16. pp. 2097–2109. Pergamon Press 1973. Printed in Great Britain

TAYLOR STABILITY OF VISCOUS FLUIDS WITH APPLICATION TO FILM BOILING

VIJAY K. DHIR and JOHN H. LIENHARD

Boiling and Phase-Change Laboratory, Mechanical Engineering Department, University of Kentucky, Lexington, Kentucky 40506, U.S.A.

(*Received* 22 *January* 1973)

Abstract—The dispersion relation is evaluated numerically for Taylor waves in a viscous unstable interface with surface tension. The solution takes account of transverse curvature and the numerical evaluations apply to horizontal cylindrical, as well as to plane, interfaces. The result is verified with frequency and wavelength data obtained during film boiling on horizontal wires. A very general empirical correlation is given, *en passant*, for the vapor blankèt thickness during film boiling.

NOMENCLATURE

A_f, A_g, B_f, B_g, undetermined constants (see equation (9) and context);
B, ratio of viscous to surface-tension forces (see equation (28));
Bo, Bond number, $R_c'^2$;
C, dimensionless group defined on abscissa of Fig. 7;
c_v, vapor specific heat at constant volume;
d, depth of fluid layer;
g, gravitational acceleration;
h_{fg}, h_{fg}^*, latent heat of vaporization. Asterisk denotes product of h_{fg} and a correction for sensible heat;
K, dimensionless wave number (see equation (19));
k, wave number, $2\pi/\lambda$;
M, dimensionless liquid viscosity parameter (see equation (21));
m, $\sqrt{(k^2 + \rho\omega/\mu)}$;
p, p_0, pressure at liquid–vapor interface. Subscript, 0, denotes pressure in undisturbed interface;
q, heat flux;
R, R_c, radius of heater. Subscript denotes radius of interface equal to $R + d_g$;
R', R_c', R and R_c multiplied by $\sqrt{[g(\rho_f - \rho_g)/\sigma]}$;
Re, a kind of Reynolds number defined by equation (29);
t, time;
u, v, velocity components in x and y directions;
x, y, coordinates parallel with, and normal to, undisturbed interface;
Γ, $(\rho_f - \rho_g)/(\rho_f + \rho_g)$;
Δ, d_g/R,
Δp_{tr}, contribution of radial or transverse curvature to the deviation of the pressure in the vapor, from that which exists when the interface is undisturbed;
ΔT, temperature difference between heater and saturated liquid;
η, y-coordinate of interface;
Λ, $1/((\sqrt{3})K)$;
λ, λ_d, wavelength. Subscript denotes λ for which the growth rate is maximum;
μ, viscosity;
ρ, density;
σ, surface tension;
φ, potential function;
ψ, perturbation function;

Ω, dimensionless growth rate (see equation (18));

$\omega, \omega_d, \omega_{d_F}$, growth rate of a wave. If ω is imaginary it will be a cyclic frequency, so ω is also called a "wave frequency". Subscript, d, denotes the "most dangerous" frequency or maximum growth rate. Subscript, F, denotes ψ_d for a plane interface.

General subscripts

f, g, denote properties of liquid and vapor regions, respectively;

x, y, t, denote partial differentiation with respect to x, y and t, respectively.

INTRODUCTION

AN UNDERSTANDING of Taylor wave behavior is important to a variety of physical processes. These include film boiling heat transfer, predictions of the peak pool-boiling heat flux, the clinging of liquids to the underside of solid surfaces as might occur during film condensation, and so forth. While Taylor waves have been treated for a variety of configurations in inviscid liquids, we lack practical solutions for the case in which the liquid is viscous.

G. I. Taylor [1] first discussed the instability of the horizontal interface between two ideal incompressible fluids of infinite depth. Bellman and Pennington [2] extended the problem by showing how to account for the interfacial surface tension and fluid viscosities. They gave closed-form expressions for the dispersion relation in inviscid fluids. They were unable to obtain a closed-form solution for the more general problem in which both viscosity and surface tension were considered, and they did not consider curvature of the interface. Several investigators have considered the plane viscous interface subsequently, but usually with an eye toward solving the dispersion relation analytically. This kind of work is typified by Willson's study [3] which extends previous efforts and presents less restrictive approximations than his predecessors.

In 1963, both Lienhard and Wong [4] and Lee [5] showed how to treat cases in which the interface was a horizontal cylinder. Lienhard and Sun [6] greatly expanded the experimental verification of the inviscid prediction for this configuration, and showed how the shape of the dispersion relation determined the scatter of wavelength data.

Our aim in this study is simply to solve the dispersion relation numerically for Taylor waves in viscous fluids including surface tension. We shall do this for both horizontal-cylindrical and plate interfaces. By going directly to numerical solutions we shall avoid the sort of restrictions (e.g. equal, or a weighted average of, viscosities in both fluids) that have robbed analytical studies of much usefulness. We shall also be able to include the effects of surface tension, curvature, and viscosity simultaneously.

Secondly, we aim to provide the first experimental verification of the predicted viscous effects in a system of practical importance.

The major restrictions of the present study will be: (1) only Newtonian and incompressible liquids will be considered, and (2) only 2-dimensional waves will be analyzed. The latter assumption will only be of concern in the plane interface situation, and here there are two pieces of evidence which support it: Squire [7] showed long ago that 3-dimensional waves are generally more stable than 2-dimensional waves in a homogeneous viscous flow. More recently Sernas [8] analyzed the Taylor instability of an inviscid plane interface and discovered that the length of the individual superposed wave components were longer and slower (i.e. they were less instable as Squire's results imply that they should be). Interestingly, Sernas' waves still defined a square grid whose spacing was equal to the two dimensional wavelength.

ANALYSIS

Figure 1a shows the idealized interface be-

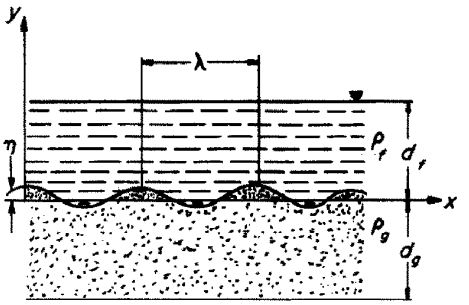

FIG. 1a. Interface between two incompressible viscous fluids of infinite depth.

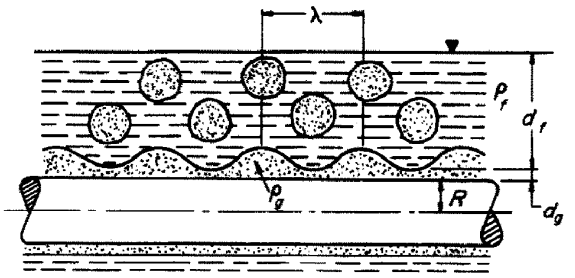

FIG. 1b. Schematic diagram of a typical configuration of film boiling on cylinders.

tween gas or vapor, and liquid, regions of arbitrary depth. Figure 1b shows a typical physical situation to which we shall subsequently show that the analysis can be applied. We shall begin by treating the plane interface, and will then show how to account for tangential curvature in the analysis. The 2-dimensional linearized equations governing the motion in either phase are:

$$u_x + v_y = 0 \tag{1}$$

$$u_t = -\frac{1}{\rho}p_x + \frac{\mu}{\rho}(u_{xx} + u_{yy}) \tag{2}$$

$$v_t = -\frac{1}{\rho}p_y - g + \frac{\mu}{\rho}(v_{xx} + v_{yy}) \tag{3}$$

where x, y and t are the coordinates parallel and normal to the interface, and time, respectively; u and v are the x and y velocity components; and ρ, g and μ, are the fluid density, the gravity, and the fluid viscosity, respectively.

These equations are satisfied by a potential function, φ, and a perturbation function, ψ, of the form

$$u = -\varphi_x - \psi_y \tag{4}$$

$$v = -\varphi_y + \psi_x \tag{5}$$

and a pressure, p, at the interface equal to

$$p = p_0 - \rho g y + \rho\varphi_t \tag{6}$$

where p_0 is the pressure in the undisturbed interface. The two functions φ and ψ must satisfy the relations

$$\varphi_{xx} + \varphi_{yy} = 0 \tag{7}$$

and

$$\frac{\mu}{\rho}(\psi_{xx} + \psi_{yy}) = \psi_t. \tag{8}$$

Using subscripts f and g to designate the liquid and gas phases, respectively, we assume perturbation and potential functions of the form:

$$\left.\begin{aligned} \psi_f &= B_f e^{-m_f y + \omega t}\sin kx \\ \varphi_f &= A_f e^{-ky + \omega t}\cos kx \\ \psi_g &= B_g e^{m_g y + \omega t}\sin kx \\ \varphi_g &= A_g e^{ky + \omega t}\cos kx \end{aligned}\right\} \tag{9}$$

where k is the wave number, ω is the growth rate, the A's and B's are undetermined constants, and (in either phase)

$$m^2 = k^2 + \rho\omega/\mu. \tag{10}$$

The real part of m must be positive so the velocity stays finite far above or below the interface.

Considering that waves of height $y = \eta(x, t)$ are propagated, we obtain for the linearized kinematic condition at the interface:

$$\eta_t = v_f \tag{11}$$

so

$$\eta = \frac{k(A_f + B_f)}{\omega}e^{\omega t}\cos kx. \tag{12}$$

The boundary conditions at the interface, i.e. at $y = \eta$, are:

$$\left.\begin{aligned} u_f &= u_g \\ v_f &= v_g \\ -p_f + 2\mu_f(v_f)_y &= -p_g + 2\mu_g(v_g)_y \\ &\quad - \sigma\eta_{xx} - \Delta p_{tr} \\ \mu_f[(v_f)_x + (u_f)_y] &= \mu_g[(v_g)_x + (u_g)_y] \end{aligned}\right\} \quad (13)$$

Equations (13) are the same as used by Bellman and Pennington with the exception of the Δp_{tr} term in the vertical force balance. This term represents the effect of transverse surface tension treated as an x-dependent contribution of an increment of pressure. In the present study we shall restrict consideration to the film boiling situation, and treat a horizontal gas cylinder in a large liquid bath, as suggested by Fig. 1b.

Since we only need to treat the stability of that portion of a cylindrical interface at the top, we base Δp_{tr} on the transverse curvature on top. Following the simple calculation made by Lienhard and Wong, we assume that the cross-section of the interface is always a circle centered on the cylinder, with its lowest point lying on a line located at $y = -2(R + d_g)$. and we obtain:

$$\Delta p_{tr} = \sigma\eta/2R_c^2 \quad (14)$$

where R_c is the actual radius of the undisturbed interface. For the film boiling situation, R_c is equal to the heater radius, R, plus the vapor depth, d_g.

The substitution of equations (9), equation (6) for both phases, and equations (12) and (14) in equations (13) gives four linear homogeneous equations in B_f, A_f, B_g and A_g:

$$\left.\begin{aligned} kA_f + m_fB_f - kA_g + m_gB_g &= 0 \\ A_f + B_f + A_g - B_g &= 0 \\ \left[\frac{g(\rho_f-\rho_g)k}{\omega} - \frac{\sigma k^3}{\omega} - \rho_f w - 2\mu_f k^2 + \frac{\sigma k}{2R_c^2\omega}\right]A_f + \left[\frac{g(\rho_f-\rho_g)k}{\omega} - \frac{\sigma k^3}{\omega} - 2\mu_f k m_f + \frac{\sigma k}{2R_c^2\omega}\right]B_f & \\ + [\rho_g\omega + 2\mu_g k^2]A_g - [2\mu_g k m_g]B_g &= 0 \\ 2\mu_f k^2 A_f + \mu_f(k^2 + m_f^2)B_f + 2\mu_g k^2 A_g - \mu_g(k^2 + m_g^2)B_g &= 0 \end{aligned}\right\} \quad (15)$$

The above equations have a non-trivial solution if and only if the determinant of the coefficient matrix is zero, i.e.

$$\begin{vmatrix} k & m_f & -k & m_g \\ 1 & 1 & 1 & -1 \\ \left\{\begin{matrix} \frac{g(\rho_f-\rho_g)k}{\omega} - \frac{\sigma k^3}{\omega} \\ -\rho_f\omega - 2\mu_f k^2 + \frac{\sigma k}{2R_c^2\omega} \end{matrix}\right\} & \left\{\begin{matrix} \frac{g(\rho_f-\rho_g)k}{\omega} - \frac{\sigma k^3}{\omega} \\ -2\mu_f k m_f + \frac{\sigma k}{2R_c^2\omega} \end{matrix}\right\} & (\rho_g\omega + 2\mu_g k^2) & -2\mu_g k m_g \\ 2\mu_f k^2 & \mu_f(k^2 + m_f^2) & 2\mu_g k^2 & -\mu_g(k^2 + m_g^2) \end{vmatrix} = 0 \quad (16)$$

Equation (16) should be valid only when the fluid depths are *infinite*. During film boiling on horizontal cylinders the depth of the vapor

blanket is *finite*, as was indicated in Fig. 1b. Recently, Hsieh [9] analyzed the inviscid instability problem in the presence of heat and mass transfer. His analysis also incorporated a finite depth of fluids. In the published discussion of his work as applied to film boiling, we showed that there was no effect of finite *vapor* depth on the "most susceptible" wavelength, while the effect on the corresponding frequency was to decrease it by only a very small amount.

The evaluation of the determinant (16) gives

$$\left[-g(\rho_f - \rho_g)k + \sigma k^3 - \frac{\sigma k}{2R_c^2} + (\rho_f + \rho_g)\omega^2\right] [\mu_f(k + m_f) + \mu_g(k + m_g)] + 4\omega k[\mu_f k + \mu_g m_g][\mu_g k + \mu_f m_f] = 0. \quad (17)$$

Our next step is to put (17) in a more usable form, so that it can be solved explicitly for frequency and wave number, or wavelength. The vapor viscosity μ_g is much less than μ_f so it may be neglected in comparison to liquid viscosity. Thus we may write, for the growth rate, $\omega = f(\rho_f + \rho_g, \rho_f - \rho_g, \mu_f, \sigma, k, g, R_c)$. This expression relates eight quantities which are expressible in three dimensions. Using the Buckingham Pi-Theorem, we can recast this problem in terms of five dimensionless groups. For these groups we choose:

(i) a dimensionless growth rate or "frequency"

$$\Omega \equiv \omega[\sigma/g^3(\rho_f - \rho_g)]^{\frac{1}{4}} \quad (18)$$

(ii) a dimensionless wave number

$$K \equiv k[\sigma/g(\rho_f - \rho_g)]^{\frac{1}{2}} \quad (19)$$

or a dimensionless wavelength, Λ, defined as

$$\Lambda = 1/((\sqrt{3})K) \quad (20)$$

(iii) a dimensionless liquid viscosity parameter

$$M \equiv \frac{\rho_f \sigma^{\frac{1}{2}}}{\mu_f g^{\frac{1}{4}}(\rho_f - \rho_g)^{\frac{1}{4}}}. \quad (21)$$

The square of this group is very nearly the Borishanski number, N, which is well known in boiling.

(iv) a dimensionless density

$$\Gamma \equiv (\rho_f - \rho_g)/(\rho_f + \rho_g) \quad (22)$$

(v) a non-dimensional cylinder radius

$$R_c' \equiv R_c[g(\rho_f - \rho_g)/\sigma]^{\frac{1}{2}}. \quad (23)$$

This number is related to the Bond number, Bo, by $Bo \equiv R_c'^2$.

Using these dimensionless numbers, we obtain the desired dispersion relation from equation (17) in dimensionless form:

$$1 - K^2 + \frac{1}{2Bo} - \frac{\Omega^2}{\Gamma K} + \frac{K}{(K^2 + \Omega M)^{\frac{1}{2}}} - \frac{K^3}{(K^2 + \Omega M)^{\frac{1}{2}}} - \frac{\Omega^2}{\Gamma(K^2 + \Omega M)^{\frac{1}{2}}} - \frac{4\Omega K}{M\Gamma} + \frac{K}{2Bo(K^2 + \Omega M)^{\frac{1}{2}}} = 0. \quad (24)$$

From (24) it is clear that when the wave growth rate is zero, there is no effect of liquid viscosity on the critial wavelength. Furthermore, when $M \to \infty$ (i.e. the liquid is inviscid) equation (24) reduces to Lienhard and Wong's expression for the inviscid case.

We are interested in the "most susceptible frequency", or the maximum growth rate, ω_d, of the disturbance (i.e. the one for which $d\Omega/dK = 0$). Differentiating (24) with respect to K and setting $d\Omega/dK = 0$, gives a second equation for the dimensionless maximum growth rate, Ω_d. Thus we have two nonlinear equations, each in two unknowns: Ω and K, and Ω_d and

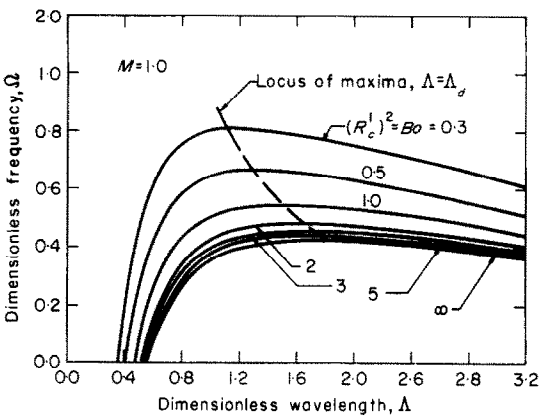

FIG. 2. Effect of radius on dispersion relation for cylinders.

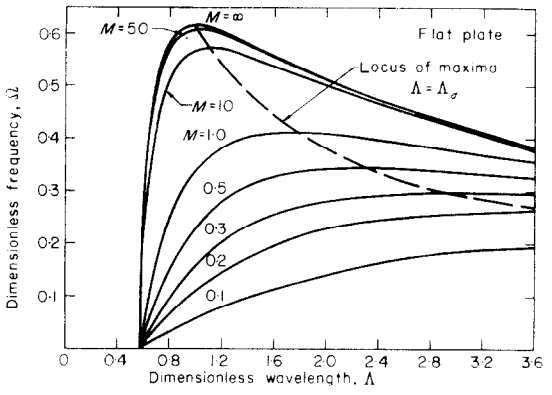

FIG. 3. Effect of viscosity on dispersion relation for a flat plate.

K_d. The two equations were solved numerically on an IBM/360 computer.

For the physical cases that we shall consider subsequently, Γ is approximately 0·9995, so we have used this value in the calculations. We might just as well have set $\Gamma = 1$, however, since Γ would have to be much farther from unity to alter the computations noticeably.

Figures 2 and 3 show the effect of Bond number and liquid viscosity separately on the dispersion relation. Figure 2 shows that transverse curvature of the cylindrical heater reduces the "most susceptible" wavelength and increases the frequency at a particular value of M. Figure 3 shows that apart from increasing the wavelength, viscosity also tends to increase the region of near-neutral stability slightly. By "region of near-neutral stability" we mean the range of wavelengths that can exist within any specified range of frequency close to the maximum frequency.

The "most susceptible frequency", and corresponding wavelength are plotted in Figs. 4 and 5, respectively, as a function of the viscosity parameter M and Bond number, Bo. As evident from these figures, the effect of liquid viscosity is to increase the wavelength and to decrease the corresponding frequency.

EXPERIMENTAL DETERMINATION OF VAPOR BLANKET THICKNESS, WAVELENGTH, AND GROWTH RATE

An experimental program was carried out to observe the wavelength, its rate of growth, and the thickness of the vapor blanket surrounding the wire heater during film boiling in viscous liquids. Since the viscosity of most of the liquids is fairly low when they boil at normal pressures, the experiments had to be performed at very low pressures to display significant viscous effects. Reagent-grade cyclohexanol, $CH_2(CH_2)_4CHOOH$, was well suited for the purpose and was used in nearly all the experiments reported here. Complete information

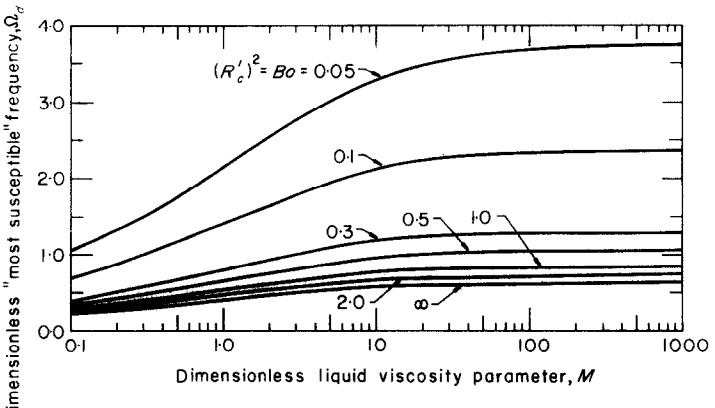

FIG. 4. Variation of Ω_d with M for various Bond numbers.

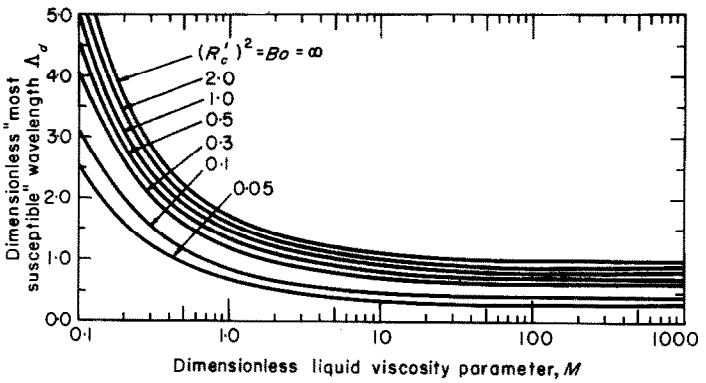

FIG. 5. Variation of Λ_d with M for various Bond numbers.

regarding the relevant physical properties of cyclohexanol, as well as full details of the experiment are given by Dhir [10].

The cylindrical test heaters were contained in an insulated brass test capsule, 8·9 × 8·9 × 17·8 cm, with glass windows in the sides. An electric preheater and 0·63 cm dia brass holders to support the test heaters were fitted to the capsule. Nichrome wires were used as test heaters and connected to the holders through small copper leads attached so as to minimize end effects. A 2·54 cm marker was mounted on the bottom of the capsule to provide a reference dimension for the reduction of photographic data.

Figure 6 shows a schematic diagram of the apparatus. A.C. power was employed in most of the experiments. The power supply to the wire was calculated from the measured current and voltage in the wire. A mercury manometer or a vacuum gage was used to note pressure inside the capsule. This pressure was corrected to take into account the head of liquid above the wire. An identical apparatus was used by Lienhard and Sun to make similar measurements and they give full details of experimental procedure.

Nichrome wires, about 10 cm long, were cleaned with soap and hot water to remove any grease or oily matter and then rinsed with the test liquid. The wire surfaces were smooth and had a cold-rolled finish. The capsule was filled with test liquid to about 2·5 cm above the wire. The vacuum pump was started and the preheater

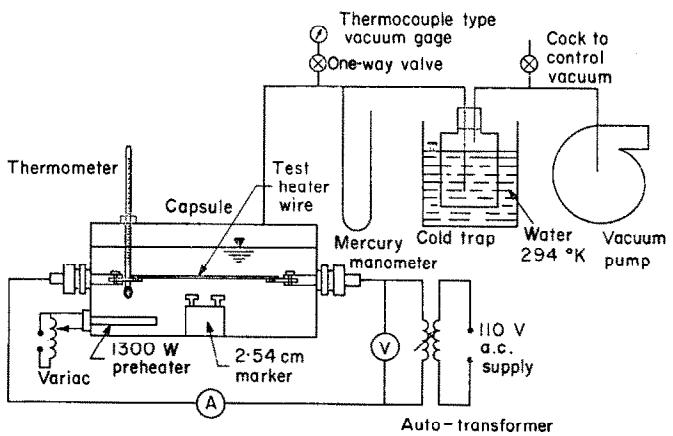

FIG. 6. Schematic diagram of the apparatus.

was used to heat the liquid to saturation temperature. The preheater was turned off before energizing the wire to avoid effects of convective currents and electric fields.

The current in the wire was steadily increased until the peak heat flux was reached and the transition from nucleate to film boiling was observed. Thereafter the current was reduced until film boiling started to disappear at the ends. This insured that the heat flux was close to minimum. Still pictures of the film boiling phenomenon were taken and observations of the liquid temperature and pressure were also made.

This procedure was repeated for wires of different sizes and at various pressures. Each time a new wire was used, the liquid in the capsule was also replaced. In some cases high speed movies were made to facilitate study of the growth rate of the disturbance.

Photographic information was used to make three different kinds of observations.

Wavelength measurements

Wavelengths were scaled from the still photographs. Care was taken to avoid situations where the merging of adjacent bubbles occur. A general deformation of the interface may be caused by the propagation of such disturbances along the wire, or local deformations may be caused by oscillations generated when outgoing bubbles separate from the interface. The probable error in the measurements of the shortest wavelengths was only about $\pm 4{\cdot}5$ per cent. The error was less for larger wavelengths.

Vapor blanket thickness measurements

In film boiling, a vapor blanket of finite thickness always surrounds the heater and there is no liquid contact with the surface of the heater. For the application of the theory developed in the previous section, we must obtain the corrected radius of the heater wire by adding the minimum blanket thickness, d_g, to R to get R_c.

To observe the vapor blanket thickness, representative pictures of film boiling were enlarged. The minimum diameter of the vapor blanket surrounding the wire was measured, using the 2·54 cm marker as a reference. The wire diameter was subtracted from this measurement to give twice the vapor blanket thickness.

Measurements of growth rate of disturbance

Hycam movies were viewed on a microfilm viewer. Starting with a frame in which a bubble had just broken away from the interface, the height of the interface was measured from the lowest boundary of the vapor blanket. Sometimes a cusp appeared on the blanket in the wake of a departing bubble, and we have ignored it. Later, the minimum diameter of the vapor blanket tube surrounding the wire was subtracted from each of the above observations to give the amplitude of the wave.

The minimum height of the interface, d_g, was used as a reference dimension for obtaining dimensionless amplitude. Thus, at a particular value of x, say $x = 0$, one may write

$$\frac{\eta}{d_g} = \exp(\omega t) = \exp\{\Omega t \sqrt[4]{[g^3(\rho_f - \rho_g)/\sigma]}\} \quad (25)$$

but we can easily show that $\sqrt{[g^3(\rho_f - \rho_g)/\sigma]} = 1{\cdot}612\omega_{d_F}$, so

$$\ln\left(\frac{\eta}{d_g}\right) = \Omega(1{\cdot}612\omega_{d_F} t) \quad (26)$$

where ω_{d_F} is the "most susceptible" frequency (or growth rate) for the disturbance in the inviscid fluid in the absence of any curvature of the heater. In all cases the dimensionless amplitude was plotted against dimensionless time, $\omega_{d_F} t$, on semi-logarithmic graph paper. The slope of the curve at any instant gave the dimensionless frequency, Ω. The probable error in the observation of the linear growth rate was ± 10 per cent.

Now we would like to compare the experimental observations of wavelength and frequency with the theoretical predictions. However, before we can do this it is necessary to present some sort of correlation for vapor

blanket thickness, because the wire radius has to be corrected for it.

VAPOR BLANKET THICKNESS CORRELATION

Baumeister and Hamill [11], while analyzing heat transfer from wires in film boiling, developed an expression for vapor blanket thickness. Their theoretical model for the film boiling configuration was a fairly approximate one; a sequence of spherical domes connected by annular passages. Neglecting inertia, they solved the equations of motion and energy with the assumption that the heat-transfer rate is maximum.

Their theoretical expressions for the vapor blanket thickness and the heat transfer coefficient can be combined to give

$$\frac{d_g}{R} = \exp\left\{7{\cdot}05\left[\frac{q\mu_g}{h^*_{fg}\rho_g\sigma}\right]^{\frac{1}{3}}\left[\frac{1}{1+9R'^2(1+d_g/R)^2}\right]^{\frac{1}{3}}\right\} - 1 \qquad (27)$$

where q is the heat flux, h^*_{fg} is the latent heat, g_{fg}, multiplied by a sensible heat correction: $[1 + 0{\cdot}34\, c_v\Delta T/h_{fg}]^2$, and c_v is the specific heat at constant volume for the vapor. A comparison of (27) with existing d_g data showed that the equation generally gives values that are too high. Therefore we sought to take a new look at the various factors influencing d_g.

The vapor blanket thickness will primarily depend on seven additional independent variables, q, ρ_g, h^*_{fg}, $g(\rho_f - \rho_g)$, σ, μ_g and R. The heat flux, q, is imagined to be transferred by conduction and used fully in the phase transformation. The eight variables can be written in four dimensions. Thus, in accordance with Buckingham Pi-Theorem, we expect the problem to be reducible to a relation among four dimensionless groups. For these we choose:

(i) The dimensionless vapor blanket thickness, $\Delta \equiv d_g/R$

(ii) The Bond number, Bo

(iii) A ratio of viscous to surface tension forces,

$$B \equiv \frac{q\mu_g}{\rho_g h^*_{fg}\sigma} \qquad (28)$$

(iv) A ratio of inertial to viscous forces—a kind of Reynolds number based on the vapor velocity,

$$Re \equiv \frac{qR\Delta}{\mu_g h^*_{fg}}. \qquad (29)$$

Baumeister and Hamill's equation involved the first three groups but the fourth group was missing because they neglected inertial terms in their equation of motion. Their assumption was realistic as long as either the wire radius, or the heat flux, or the vapor blanket thickness is small; but the ratio of inertial to viscous forces

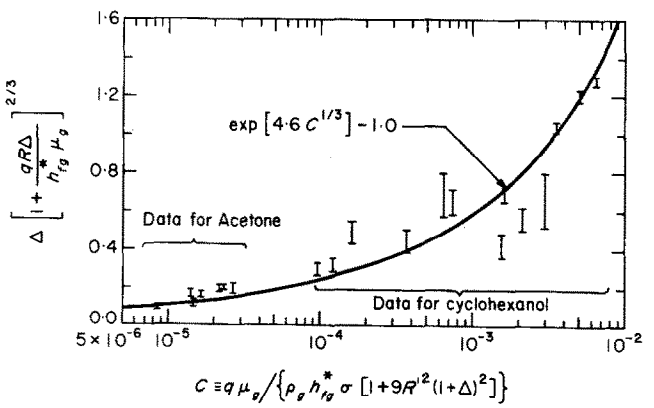

FIG. 7. Correlation for vapor blanket thickness.

might be of the order of magnitude of unity when the heat flux is high or the vapor blanket thickness is large.

In Fig. 7, we have plotted 20 data points for vapor blanket thickness on wires in the range $0{\cdot}11 \leqslant R' \leqslant 0{\cdot}65$ during the film boiling of acetone and cyclohexanol. While the abscissa is the same as Baumeister and Hamill's, the vapor blanket thickness has been correlated with the Reynolds number as an additional parameter. This correction has been obtained by a trial and error procedure and no theoretical reason is offered for taking the exponent in the inertia correction term to be 2/3. In forming the vapor blanket thickness correlation, all of the vapor properties have been evaluated at the mean film temperature and all radiant heat flux is assumed to generate vapor. The raw data are given by Dhir [10].

The group, $qR\Delta/\mu_g h^*_{fg}$, varied approximately from 0·2 to 2·5 in all the observations. Smaller values of this group usually occur near the left hand side of the figure. The data scatter represents minimum and maximum measurements of vapor blanket thickness. The accuracy of these measurements is ± 10 per cent. The data are correlated well by the solid line whose governing equation is:

$$\Delta = \frac{\left\{4{\cdot}60\left[\frac{q\mu_g}{\rho_g h^*_{fg}\sigma}\right]^{\frac{1}{3}}\left[\frac{1}{1+9R'^2(1+\Delta)^2}\right]^{\frac{1}{3}}\right\} - 1}{\left[1+\frac{qR\Delta}{u_g h^*_{fg}}\right]^{\frac{2}{3}}}$$

COMPARISON OF WAVELENGTH PREDICTIONS WITH EXPERIMENT

Observed wavelengths for cyclohexanol boiling at a temperature of 302·5°K, corresponding to a pressure of 0·296 kPa, are displayed in Fig. 8. The value of the liquid viscosity parameter, M, is close to 5. The theoretical prediction for the viscous and inviscid cases is also shown in the figure. The wire radius has been corrected to R_c to take into account the thickness of the vapor blanket surrounding it. The raw wavelength data are given by Dhir.

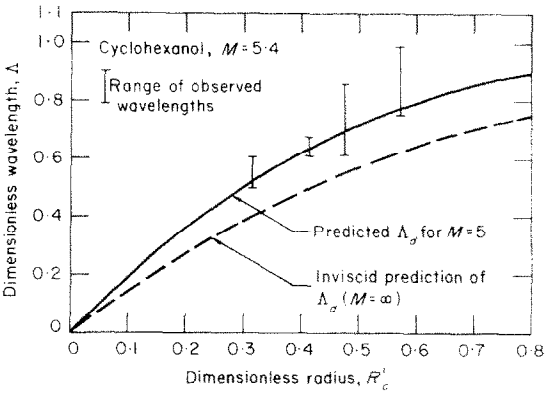

FIG. 8. Wavelengths on horizontal cylinders.

Although wavelengths were measured for various heat fluxes, those displayed in Fig. 8 correspond to the lowest heat flux. This is done to avoid the longer wavelengths which may, as we will see shortly, be favored at higher heat fluxes. The data show a wide variability, but the lowest points in the range of the data scatter do embrace the theoretical prediction which takes the dominant wavelength to be the "most susceptible" one. The inviscid predictions would have suggested wavelengths about 28 per cent too short.

Figure 9 shows photographs of film boiling for two of the data points in Fig. 8. Although there is slight phase difference across the length of the wire, the Taylor wave is very well developed. The bubble release pattern is good. The

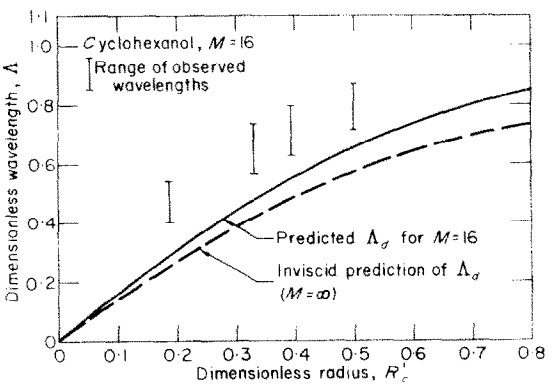

FIG. 10. Wavelengths on horizontal cylinders.

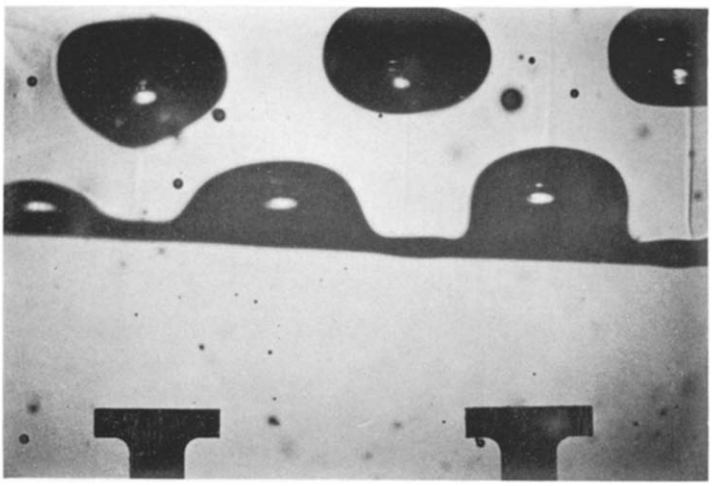

$R' = 0{\cdot}23$ $R'_c = 0{\cdot}33$

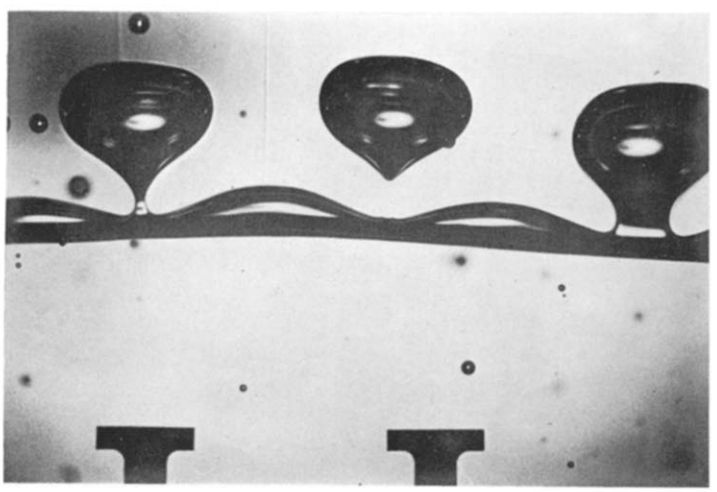

$R' = 0{\cdot}34$ $R'_c = 0{\cdot}43$

FIG. 9. Film boiling of cyclohexanol. $M = 5{\cdot}4$.

process is slower and viscosity seems to have dampened the small interfacial disturbances which may be observed in less viscous liquids.

Wavelength data for $M = 16$ are plotted in Fig. 10. Here the absolute pressure is 1·06 kPa and the saturation temperature is 329°K. In this case, observed wavelengths are higher and the data again show wide variability. This variability in data can be explained from the dispersion relation shown in Fig. 2. Near the maximum frequency there is a wide region of near-neutral stability. Thus, for frequencies slightly less than the maximum, a large range of wavelengths close to λ_d is possible.

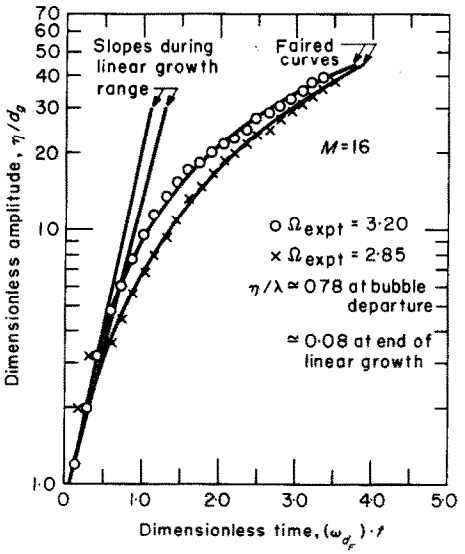

FIG. 11. Growth of waves on a 0·51 mm dia wire heater in cyclohexanol. P — 1·06 k Pa, $q = 0{\cdot}86 \times 10^5$ W/m², $f_b = 20$ bubble/s, $\omega_{d_F} = 45{\cdot}5$ Hz, $R' = 0{\cdot}14$, $R'_c = 0{\cdot}22$.

COMPARISON OF WAVE GROWTH RATE PREDICTIONS WITH EXPERIMENT

Figure 11 shows plots of dimensionless wave amplitude vs time on semi-logarithmic coordinates for a typical value of R'. The liquid viscosity parameter, M, is 16. The data are for two randomly-picked, regularly-growing waves during 5–10 s of motion pictures of film boiling.

This figure and many others like it reveal that

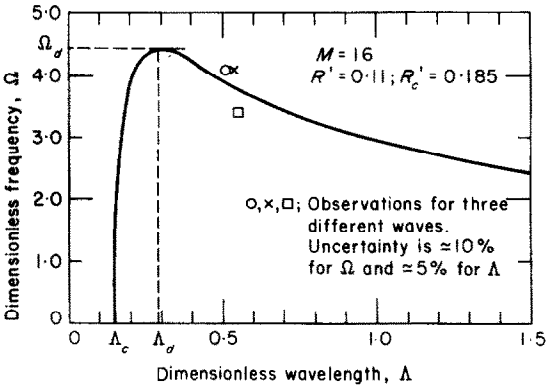

FIG. 12. Experimental verification of dispersion relation for cyclohexanol at 1·06 k Pa. $q = 0{\cdot}85 \times 10^5$ W/m².

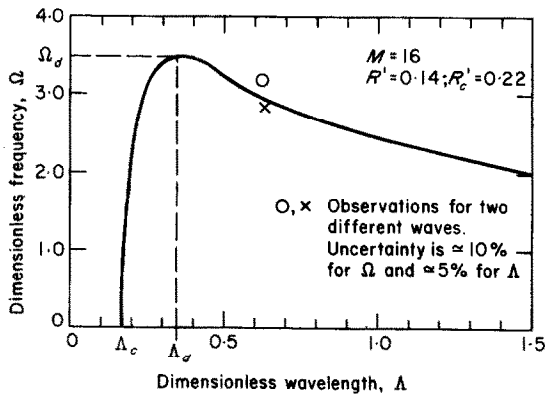

FIG. 13. Experimental verification of dispersion relation for cyclohexanol at 1·06 k Pa. $q = 0{\cdot}86 \times 10^5$ W/m².

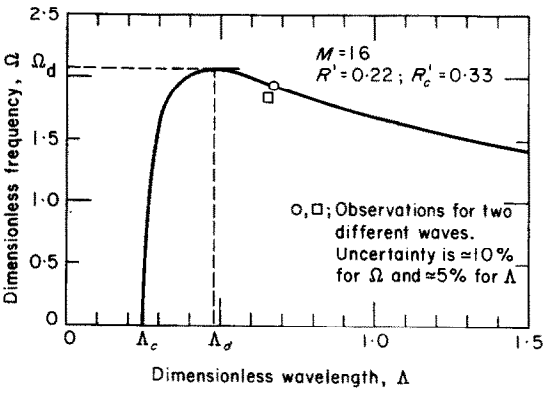

FIG. 14. Experimental verification of dispersion relation for cyclohexanol at 1·06 k Pa. $q = 1{\cdot}01 \times 10^5$ W/m².

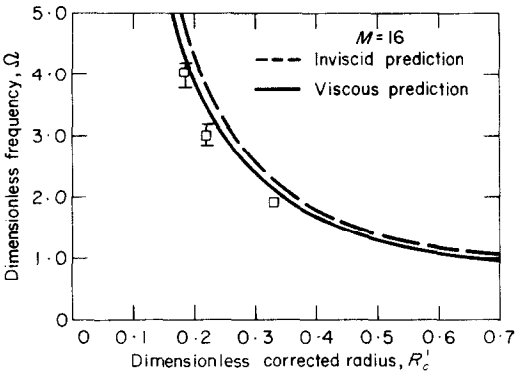

FIG. 15. Experimental observation of frequency of dominant wavelength on cylinders.

bubbles grow linearly during the first 12 per cent or so of growth. This is the period during which we would expect our linearized theoretical predictions of the frequency to be valid. We note that the bubble grows in height to about 78 per cent of the wavelength before it leaves the interface.

In Figs. 12–14, we trace the dispersion relations for three dimensionless corrected radii and $M = 16$, and we display the experimental points obtained as in Fig. 11 on them. The relation between wavelength and frequency is borne out well in each case. It is clear that wavelengths with frequencies slightly less than the "most susceptible" frequency can easily occur. In Fig. 15, observed frequencies are plotted as a function of R_c' along with the viscous and inviscid ($M \to \infty$) predictions. The data fall slightly below the viscous predictions, but the inviscid theory would have predicted still higher frequencies.

The growth rates for some values of M in excess of 50 are compared with the inviscid limit in Fig. 16. The comparison is very satisfactory. That the growth rates do not exceed the maximum possible value of Ω is encouraging, since we have already seen that Ω should be equal to or slightly less than its maximum value.

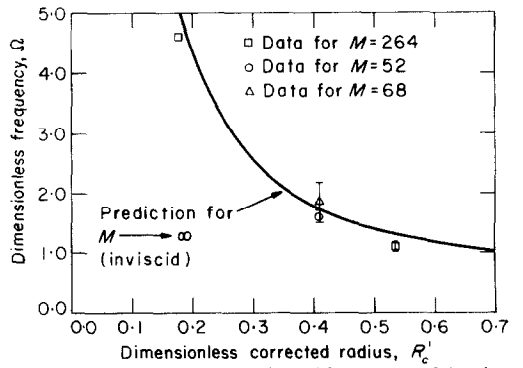

FIG. 16. Experimental observation of frequency of dominant wavelength on cylinders.

CONCLUSIONS

(A) Complete numerical evaluations of the dispersion relation have been made for both plane and cylindrical, Taylor-unstable interfaces, considering both surface tension and fluid viscosity.

(B) An increase of wavelength with the liquid viscosity has been measured and found to compare well with the theoretical predictions. However, the dispersion relation permits some variability of the wavelength around the value for which the growth rate is maximum, with longer wavelengths favored. Thus some measured wavelengths exceed the "most dangerous" one.

(C) The wavelength and frequency (or growth rate) measurements are faithful to the predicted dispersion relation.

(D) A correlation for the vapor blanket thickness around a cylindrical heater has been established.

ACKNOWLEDGEMENT

This work was funded by NASA Grant, NGR-18-001-035, under the cognizance of Lewis Research Center. We wish to express our gratitude for their support.

REFERENCES

1. SIR G. I. TAYLOR, The instability of liquid surfaces when accelerated in a direction perpendicular to their plane, *Proc. R. Soc., Lond.* **201A**, 192 (1950).
2. R. BELLMAN and R. H. PENNINGTON, Effects of surface tension and viscosity on Taylor instability, *Q. Appl. Math.* **12**, 151–162 (1954).
3. A. J. WILLSON, On the stability of two superposed fluids, *Proc. Camb. Phil. Soc.* **61**, 595–607 (1965).
4. J. H. LIENHARD and P. T. Y. WONG, The dominant unstable wavelength and minimum heat flux during

film boiling on a horizontal cylinder, *J. Heat Transfer* **88** (2), 220–226 (1964).
5. S. L. Lee, Taylor instability of a liquid film around a long horizontal circular cylindrical body in still air, *J. Heat Transfer* **85** (3), 443–447 (1963).
6. J. H. Lienhard and K. H. Sun, Effects of gravity and size upon film boiling from horizontal cylinders, *J. Heat Transfer* **92** (2), 292–298 (1970).
7. H. B. Squire, On the stability of three-dimensional distribution of viscous fluid between parallel walls, *Proc. R. Soc., Lond.* **142A**, 621–628 (1933).
8. V. Sernas, Minimum heat flux in film boiling—a three-dimensional model, Proc., 2nd Canadian Cong. of Appl. Mech., Univ. of Waterloo, pp. 425–426 (May 1969).
9. D. Y. Hsieh, Effects of heat and mass transfer on Rayleigh–Taylor instability, *J. Basic Engng* **94** (1), 156–162 (1972).
10. V. K. Dhir, Viscous hydrodynamic instability theory of the peak and minimum pool boiling heat fluxes, College of Engineering Bulletin No. UKY-100, University of Kentucky, (1972); Ph.D. dissertation (August 1972).
11. K. J. Baumeister and T. D. Hamill, Film boiling from a thin wire as an optimum boundary-value problem, ASME Paper 67-HT-62, ASME–AIChE Heat Transfer Conference, Seattle, Washington (1967).

STABILITE DE TAYLOR POUR DES FLUIDES VISQUEUX ET APPLICATION A L'EBULLITION EN FILM

Résumé—On a évalué numériquement la relation de dispersion pour des ondes de Taylor à un interface visqueux instable avec tension superficielle. La solution tient compte de la courbure transversale et les évaluations numériques s'appliquent aux interfaces aussi bien en forme de cylindre horizontal que de plan. Le résultat est vérifié par des mesures de fréquence et de longueur d'onde faites au cours de l'ébullition en film sur des fils horizontaux. On donne une relation empirique très générale, pour l'épaisseur de la gaine de vapeur pendant l'ébullition en film.

DIE TAYLOR-STABILITÄT VON ZÄHEN FLÜSSIGKEITEN MIT ANWENDUNG AUF DAS FILMSIEDEN.

Zusammenfassung—Die Ausbreitungsbeziehung für Taylor-Wellen mit Oberflächenspannung an einer instabilen Grenzschicht wurde numerisch gelöst. Die Lösung berücksichtigt eine Krümmung in Querrichtung und die numerischen Ergebnisse passen für horizontale, zylindrische, sowie für ebene Grenzflächen. Das Ergebnis wurde bestätigt mit Frequenz- und Wellenlängenwerten aus Filmsiedemessungen an horizontalen Drähten. Eine sehr allgemeine empirische Beziehung wird angegeben zur Bestimmung der Dampfschichtdicke beim Filmsieden.

ТЕЙЛОРОВСКАЯ УСТОЙЧИВОСТЬ ПРИ ПЛЕНОЧНОМ КИПЕНИИ ВЯЗКИХ ЖИДКОСТЕЙ

Аннотация—Проводится численный расчет дисперсионного соотношения для Тейлоровских волн в нестадионарной вязкой поверхности раздела с поверхностным натяжением. Решение учитывает поперечную кривизну, и численные оценки могут использоваться для горизонтальных цилиндрических и плоских поверхностей раздела. Результаты сравниваются с измеренными значениями частоты и длины волны при пленочном кипении на горизонтальных проволоках. Приводится весьма общее эмпирическое соотношение для толщины слоя пара при пленочном кипении.